

Preparation and Photocatalytic Characterization of Modified TiO₂/Nd/rice Husk Ash Nanomaterial for Rifampicin Removal in Aqueous Solution

Thuy Dang Thi Ngoc (✉ dangngocthuy@gmail.com)

HUMG: Hanoi University of Mining and Geology

Ha Nguyen Thi

Vietnam National University University of Science

Anh Ngo Van

Vietnam National University

Sen Nguyen Thi

Institute of natural resources and environment science

Dung Nguyen Duc

Hanoi University of Mining and Geology

Nam Nguyen Hoang

Hanoi University of Mining and Geology

Research Article

Keywords: hydrothermal method, Nd, rice husk ash, rifampicin, TiO₂ nanomaterial, photocatalyst

Posted Date: July 6th, 2021

DOI: <https://doi.org/10.21203/rs.3.rs-581621/v1>

License: © ⓘ This work is licensed under a Creative Commons Attribution 4.0 International License.

[Read Full License](#)

1 **Preparation and photocatalytic characterization of modified TiO₂/Nd/rice husk ash**
2 **nanomaterial for Rifampicin removal in aqueous solution**

3
4 **Thuy Dang Thi Ngoc^{1*}, Ha Nguyen Thi², Anh Ngo Van², Sen Nguyen Thi³, Dung Nguyen Duc¹, Nam**
5 **Nguyen Hoang¹**

6
7 *¹Department of Environment, Hanoi University of Mining and Geology, No. 18 Vien street, Bac*
8 *Tu Liem district, Hanoi, Vietnam*

9
10 *²Faculty of Environmental Sciences, VNU-University of Science, Vietnam National University,*
11 *Hanoi - 334 Nguyen Trai, Thanh Xuan, Ha Noi, Vietnam*

12
13 *³Institute of Natural Resources and Environment Science, 7th floor, GIM building, 460 Lane,*
14 *Khuong Dinh St, Ha Dinh, Thanh Xuan, Ha Noi, Vietnam*

15
16
17 * Author for Correspondence:

18 Email: dangngocthuy@gmail.com; Telephone: +84 (0) 969122275

19
20 Keywords: hydrothermal method, Nd, rice husk ash, rifampicin, TiO₂ nanomaterial, photocatalyst

23 **Declarations**

24 **Ethics approval and consent to participate:** Not applicable.

25 **Consent for publication:** Not applicable.

26 **Availability of data and materials:** The data presented in this study are available on request
27 from the corresponding author. The data are not publicly available due to the information
28 security conditions of the project.

29 **Competing interests:** The authors declare that they have no competing interests.

30 **Funding:** Not applicable

31 **Authors' contributions:** Thuy Dang Thi Ngoc: makes contribution in proposing ideas and
32 designing research; experiment implementation, data collection, data analysis and translation; has
33 contributed to the drafting of the article. Nam Nguyen Hoang: makes an important contribution in
34 proposing ideas and designing research; checks data; data processing; examines the knowledge
35 content of the article; the ratification of the final draft before submitting it to the scientific journal.
36 Ha Nguyen Thi: makes an important contribution in proposing ideas and designing research;
37 checks data; data processing; seriously examines the knowledge content of the article; the
38 ratification of the final draft before submitting it to the scientific journal. Anh Ngo Van: has
39 contributed to the drafting and finalizing of the article, data processing. Sen Nguyen Thi and Dung
40 Nguyen Duc: make contribution in experiment implementation, data collection, data analysis and
41 translation.

42 **Acknowledgements:**

43 *The authors would like to sincerely thank the Institute of Biotechnology - Institute of*
44 *Environmental Technology, Vietnam Academy of Sciences; Center for Environmental Treatment -*
45 *Military Institute of Science and Technology; Department of Chemistry – Faculty of Basic Sciences*
46 *– University of Mining - Geology has facilitated and support in the research process.*

47

48

49

Abstract

50 The neodymium doping of titanium dioxide with content of Nd varying from 0.01 to 0.8%
51 was conducted by the sol-gel hydrothermic method. TiO₂/Nd is then coated on rice husk ash to
52 produce modified TiO₂/Nd/rice husk ash material using Nd content of 0.36% w/w. The materials'
53 structure characteristic and photocatalytic properties have been analyzed by the XRD, EDX, TEM,
54 SEM, forbidden zone energy (E_g) and specific surface area (BET). TiO₂/Nd material shows a
55 higher photocatalytic decomposition capacity in comparison to TiO₂ and depended on the Nd
56 content. The Rifampicin removal efficiency of TiO₂/Nd materials with Nd contents ranged from
57 0.36 to 0.80% had an increase of about 40% higher than that of TiO₂/Nd containing Nd from 0.01
58 to 0.28%. This new photocatalytic TiO₂/Nd/rice husk ash material is used to decompose
59 Rifampicin. Within 90 minutes under sunlight, the Rifampicin decomposed efficiency of TiO₂/Nd
60 and TiO₂/Nd/rice husk ash material reached about 86 and 75%, respectively. Even lower efficiency
61 was obtained, the latter material was chosen for Rifampicin residue decomposition in the water
62 under sunlight through photocatalytic process because it has some advantages such as smaller
63 amount was needed and easily to be recovered. Rifampicin removal process, k values were found
64 matching more to zero and first order kinetics. Especially, for powder TiO₂/Nd and TiO₂/Nd/Rice
65 husk ash under solar irradiation the R² reached about 0.98.

66

67 Introduction

68 Rifampicin is an antibiotic with the molecular formula C₄₃H₅₈N₄O₁₂ that works with
69 bacteria of the Mycobacterium strain, especially *M. tuberculosis*, *M. leprae* and other
70 Mycobacterium bacteria such as *M. bovis*, *M. avium*. The minimum inhibitory concentration for
71 *M. tuberculosis* bacteria are 0.1 - 2.0 micrograms/ml. The presence of particular antibiotics
72 especially Rifampicin in water has a significant influence on water treatment by biological
73 methods.

74 The removal of antibiotic residues has been of great interest to many scientists. Currently,
75 there are many methods of antibiotic residues removal such as absorption, advanced oxidation,
76 biology, photocatalyst etc. Using photocatalyst is one of the techniques that promises to
77 decompose not only persistent organic pollutants (POPs) that are difficult to decompose by
78 biological methods, harmful microorganisms, but also, remove some antibiotics that are difficult

79 or impossible to treat by biological methods etc. The characteristic of this type of catalyst is that,
80 under the effect of light, will produce pairs of electrons (e^-) and hole (h^+), thereby creating
81 compounds with strong oxidation properties and abundant electronic supplies (Choi,
82 Maruthamuthu et al. 2009, Yang, Doudrick et al. 2013, Saucedo-Lucero and Arriaga 2015,
83 Hajizadeh, Amin et al. 2018).

84 Nano TiO_2 has widely used because of its photochemically stable, photocatalytic property,
85 low cost and nontoxic to human and environment. Nano TiO_2 that is used as catalyst will not be
86 converted by reactions, therefore, it is required only initial investment for long term use (Wen, Li
87 et al. 2015, Huang, Lu et al. 2017, Aregu, Asfaw et al. 2018). Therefore, nano-size TiO_2 has the
88 economical and technical advantages in inorganic, organic or microbials removal (Aregu, Asfaw
89 et al. 2018). However, due to restricted zone energy of nano-size TiO_2 is high (3,05–3,25 eV),
90 only the short wavelength radiation (< 380 nm) could activate the electron from the valence to the
91 conduction bands for photocatalytic activity (Ma, Wang et al. 2014, Wen, Li et al. 2015). Mean
92 whiles, the ultraviolet radiation in the solar radiation reaches the Earth's surface only account about
93 4 %, making the use of this natural source for the purpose of treating environmental problems with
94 TiO_2 is limited (Li, Yu et al. 2015, Wen, Li et al. 2015). Therefore, it is necessary to reduce the
95 band-gap energy of TiO_2 so it has photocatalytic activity under the visible light. As a result, many
96 researches have denatured TiO_2 materials to narrow down the bending energy (E_g), to enlarge the
97 excitation light from the UV region to the visible area (Ma, Wang et al. 2014, Li, Yu et al. 2015,
98 Wen, Li et al. 2015).

99 Number of the recent surface modifications or TiO_2 structures by various methods have
100 been carried out by introducing metal ions such as Zn, Fe, Cr, Eu, Y, Ag, Ni, etc. and non-metal
101 ions such as N, C, S, F, Cl,... These materials have been shown to be effective, enhancing
102 photocatalytic activity in the visible light region (Chen and Mao 2007, Maeda and Domen 2007,
103 Du and Eisenberg 2012, Fukuzumi, Hong et al. 2013, Wanga and Astruc 2014, Li, Yu et al. 2015,
104 Wen, Li et al. 2015).

105 In addition, due to small and dispersion the TiO_2 nanoparticles is difficult to recover for
106 reuse. Therefore, to reduce the cost of products needs to attach TiO_2 nanostats to the carrier has a
107 large surface area. These carriers should have the following characteristics: good bonding to the
108 catalyst; no catalytic decomposition effect; has a large surface area; has an affinity for adsorption

109 with pollutants such as beeswax, activated carbon, glass, silica gel, polymer materials, zeolite,
110 cotton, cellulose...

111 Husk cover and rice husk ash are agricultural waste, accounting for about one fifth of the
112 world's annual production of rice (about 545 million tons per annum). Globally, there are more
113 than twenty million tons of husk ash released each year (General statistics office 2018). The
114 amount of ash that enters the ecosystem can be damaging to humans and animals, such as silicosis,
115 respiratory failure, and death. Husk ash is used as a good adsorbent for the treatment of many
116 inorganic and organic pollutants (Liu, Guo et al. 2011, Kumar, Sengupta et al. 2015, Zhang, Ding
117 et al. 2015). Therefore, solves a part of agricultural waste, reducing the amount of waste rice husk
118 (Liu, Guo et al. 2011). In addition, husk ash is also used as a carrier for catalytic materials because
119 it has a good mechanical stability, are chemically inert, when used as a carrier will facilitate the
120 separation of catalyst from the solution after reaction. The application of this material is that
121 absorbing nitrogen compounds like Rifampicin (Kumar, Singha et al. 2015).

122 Thus, utilizing rice husk ash and adsorbents of nitrogen - containing organic compounds
123 such as Rifampicin, coupled with photochemical capacities of TiO₂ nanoparticles photochemical
124 catalysts for the transfer of Rifampicin to CO₂, H₂O, N₂ (non-toxic). One that solves the problem
125 of minimizing environmental pollution from agricultural waste, on the other hand increases the
126 efficiency of nanomaterials as well as saves on materials and does not require post-processing
127 solutions. It opens up a new way of handling nitrogen compounds as well as can be applied in
128 industry (Cong, Zhang et al. 2007).

129 **Experiment**

130 *Chemicals and equipment*

131 Chemicals used in research include: TiCl₄, NH₄NO₃, PVA, (NH₂)₂CO, Rifampicin (see
132 Figure 1), Methanol, H₂SO₄, HNO₃, Na₂CO₃, NaOH, NaH₂PO₄, Na₂HPO₄, NdCl₃. The chemical
133 compounds have a purity of PA, produced by the Merck, German, distilled water and super
134 distilled water.

135 **Figure 1.** The chemical structure of Rifampicin

136 Husk is taken from the Rice enterprise in Hoai Duc, Ha Noi. The rice husk is washed with
137 distilled water to remove impurities, dried at 105°C for 2 hrs., then put in furnace at temperatures
138 of 800°C for 3 hrs. in N₂ gas environment to have ash bearing material. The product after furnace
139 is grinded to the size of about 0.1-0.5 mm.

140 Water samples: water sample containing Rifampicin is prepared with Rifampicin
141 concentration 20 mg/L. TiCl_4 0.5M was prepared from TiCl_4 3M by diluted using cold water.

142 Buffer solution of phosphate pH 7.4 is prepared from the NaH_2PO_4 and Na_2HPO_4 .

143 Instruments were used to perform experiments consist of: Drying cabinet produced by
144 Germany; oven Carbolite model AAF-11/7 produced in England. Heating magnetic stirrer IKA by
145 Germany.

146 ***Preparation of modified TiO_2/Nd nanomaterial coated in husk ash by the sol-gel hydrothermal*** 147 ***method***

148 *Preparation of modified TiO_2/Nd nanomaterial by the sol-gel hydrothermal method*

149 TiO_2 nanomaterial modified Nd was prepared by the sol-gel hydrothermal method
150 according to Nguyen H.N. et al (2016): Mixing 60 ml NH_4NO_3 1M with 450 ml $(\text{NH}_2)_2\text{CO}$ 1M +
151 180 ml PVA 1M + 60ml TiCl_4 (0,5M) + from 0.1 to 1.0 ml (1g/L); heating to 70°C , stirring
152 continuously in 24 hrs., 1200 rpm, then heating up to 90°C , and stirring for 12 hrs. Sol-gel solution
153 obtained was dried at 120°C for 12 hrs., then the temperature was increased to 250°C for 3 hrs.
154 until no more white smoke was released, and black powder was generated. Finally, materials were
155 put in furnace at 600°C for 3 hrs. with a heating rate of $10^\circ\text{C}/\text{min}$. Materials after the furnace were
156 washed 4-5 times with distilled water and super clean water, then dried at 120°C for 2 hrs (Nam,
157 Hiep et al. 2016).

158 **Table 1.** Composition and rate of chemicals prepared nano TiO_2 modified Nd by the sol-gel
159 hydrothermal method

160 *Coating TiO_2/Nd nanomaterial on rice husk ash*

161 Husk ash was added into sol-gel solution prepared in section 2.2.(a) to have the
162 concentrations of TiO_2/Nd in husk ash corresponding 0.1; 0.2; 0.3; 0.4 and 0.5% w/w. The thermal
163 modification process started with well stirring the mixture at 90°C for 12 hrs. then was followed
164 by similar processes as in the preparation of Nd modified TiO_2 nano-materials in section
165 “*Preparation of modified TiO_2/Nd nanomaterial by the sol-gel hydrothermal method*”.

166 ***Rifampicin removal of TiO_2/Nd nanomaterial and TiO_2/Nd nanomaterial/husk ash***

167 Put 0.1g of powdered TiO_2/Nd nano-material or 1.0g TiO_2/Nd nanomaterial/husk ash in
168 200ml glass cups, add 100 ml of Rifampicin solution at 20 mg/L, stirring the solution at 100 rpm.
169 Experiments were conducted under natural light (day and night). The natural light has illumination

170 intensity of 20.000 Lux. Samples were taken at 0, 15, 30, 45, 60, 75 and 90 minutes to analyze
171 residual Rifampicin concentration.

172 ***Analysis methods***

173 The surface area of the husk ash is determined by the BET analysis in N₂ environment at
174 196°C using NOVA 1200 Quanta chrome-USA. Surface structure of husk ash and TiO₂
175 material/husk ash defined by the SEM method (Jeol 5410 LV, Japan). Purity of a TiO₂ material
176 defined by X-ray diffraction method (XRD), Siemens D5005, Germany. Nano TiO₂ particle size
177 determined by TEM, LIBRA120, Germany. The element compositions are analyzed by Energy
178 dispersive analysis of X-rays (EDX), Jeol 6490JED 2300, 2300, Japan.

179 Rifampicin concentration was analyzed by molecular absorption spectroscopic method
180 according to Benetton et al. (1998). Calibration curve was prepared using UV-VIS Optizen
181 2120UV, England.

182 ***Rifampicin degradation kinetic calculations***

183 The rate of rifampicin degradation and observe the best fit indicating the reaction order
184 were investigated by plotting the remained rifampicin concentration versus time using zero-order,
185 first-order and second-order kinetic models (Vaucher, Paim et al. 2010):

186 Zero-order reaction: $C = C_0 - kt$ (1)

187 First-order reaction: $C = \ln C_0 - kt \rightarrow C = C_0 e^{-kt}$ (2)

188 Second-order reaction: $\frac{1}{C} = \frac{1}{C_0} + kt \frac{1}{C}$ (3)

189 Where: C_0 is the concentration of the reactants under consideration at time zero; C is the
190 concentration after reaction time, t ; k is the reaction rate constant.

191 Based on the obtained kinetic graphs, regression coefficients and the kinetics parameters
192 such as apparent order degradation rate constant (k) were identified.

193 **Results and discussions**

194 ***Characteristics of powder TiO₂/Nd modified material***

195 Samples of TiO₂/Nd material obtained after synthesis with different Nd contents were
196 analyzed the structure, photolysis properties and surface properties using of EDX, XRD, SEM,...
197 measurements.

198 ***Ermology of nano TiO₂/Nd modified material***

199 To analyze the size of the prepared material and their crystal forms, conduct particle size
200 analysis using TEM and XRD. The morphology of the nano TiO₂/Nd modified materials using the
201 solgel hydrothermal method is shown on Figure 2.

202 **Figure 2.** TEM image of TiO₂/Nd modified nanomaterials with different Nd content

203 Figure 2 shows that, with different Nd content the materials are even in the form of anatase
204 and has a relatively even particle size, at about <20 nm. Compared to the results of the synthesis
205 of nano materials by the solgel method (Nam, Hiep et al. 2016), the nano TiO₂/Nd modified
206 materials have the particle sizes more even and smaller than that of non-modified materials. This
207 result is also consistent with the findings of the study by Huang You et al (2006) and Nam et al.
208 (2016).

209 *The XRD spectrum of the TiO₂/Nd modified nanomaterials*

210 X-ray diffraction (XRD) patterns of the nano TiO₂ non-modified materials and the nano
211 TiO₂/Nd modified materials are shown on Figure 3. As can be seen all peaks are sharp and no
212 strange diffraction peaks appeared that prove the prepared TiO₂ materials have a characteristic
213 crystal structure. Diffraction peaks are characteristic at 2θ values about 25.36 (101), 37.93 (004),
214 48.07 (200), 54.03 (105), 55.13 (211) and 62.81 (204) show that the nano materials obtained exist
215 only in the anatase phase. In addition, no characteristic peaks of the rutile and brookite phase
216 appear.

217 **Figure 3.** XRD images of nano TiO₂/Nd modified materials with different Nd content

218 **Table 2.** Lattice parameters, particle size and density of *TiO₂/Nd* modified nanomaterials
219 with different Nd content

220 The results showed that Nd³⁺ ions were inserted in the crystal structure of nano TiO₂
221 materials. Although they are prepared with different Nd contents, the nano materials obtained are
222 pure, single-phase, without the appearance of diffraction peaks of rare earth ions. Besides, the
223 crystal lattice parameters of materials with different Nd contents there are differences in lattice
224 constants a and c, in which of nano TiO₂/Nd modified material found larger sizes than non-
225 modified materials. This can be explained, since the radius of the Nd³⁺ ion is larger in size than
226 that of the Ti⁴⁺ ion, when the Nd³⁺ ion replaces the position of the Ti⁴⁺ ion in the crystal lattice it
227 will make the crystal larger in size (El-Bahy, Ismail et al. 2009, Nguyễn Văn Hưng, Ngô Sỹ Lương
228 et al. 2012).

229 However, the size of the crystal lattice and the density of all 6 materials are almost the
230 same. In addition, these findings are similar to some previous studies where the lattice cell size of
231 the material prepared by the sol-gel hydrothermal method is smaller and the density is larger
232 when modifying by metals (Huang, You et al. 2006, El-Bahy, Ismail et al. 2009, Nguyễn Văn
233 Hưng, Ngô Sỹ Lương et al. 2012).

234 *EDX spectrum of TiO₂/Nd nanomaterials*

235 The percentages of elements contained in nano TiO₂/Nd materials with different contents
236 of Nd are in shown in Figure 4.

237 **Figure 4.** EDX images of TiO₂/Nd modified nanomaterials with different Nd contents

238 Peaks on EDX diagrams specify the presence Ti, O and Nd elements in material samples.
239 Peaks of other elements are not appeared. This proves that synthetic TiO₂ nanomaterials are highly
240 pure. The results of quantitative analysis of the material's compositions show that Ti content
241 accounts for between 46 and 57% by weight and from 27 to 31% by atomic numbers, O content
242 found in the ranges of 42-54% and 69- 78% by weight and atomic numbers, respectively. Except
243 Ti and O peaks, there was peaks of Nd, with a relatively small intensity, accounting for only 0.01
244 to 0.8% and from 0.01 to 0.14 % by weight and atomic number, respectively.

245 Nano materials are obtained evenly in single-crystal form and in the form of anatase. In the
246 crystal lattice of TiO₂, Ti atoms in some vertices are replaced by Nd atoms. However, since Ti has
247 valency IV, it will form a bond with the 4 surrounding O atoms while the Nd has valency III, so
248 when Nd is replaced in the position of the Ti atom, the Nd atom creates a electric imbalance. In
249 addition, on the surface of TiO₂ there are OH⁻ groups that produce from water separation process
250 of oxides. These groups can exist in a free or the surface bond states through hydrogen bonds.
251 That's why the TiO₂ surface form several molecular layers. The OH⁻ group can catch holes and
252 absorbed water molecules that can give electrons to form reduced hydroxyl radicals. Therefore,
253 the rate of re-combination between electron-hole pairs is reduced and the photocatalytic activity
254 of TiO₂ is enhanced when it is modified by the Nd³⁺ ion (El-Bahy, Ismail et al. 2009).

255 *Eg values of TiO₂/Nd modified nanomaterial*

256 As can be seen in Figure 5, the sample has an Nd content of 0.16% for the lowest Eg value.
257 The highest Eg value found at material with an Nd content of 0.8%, reaching 3.21 eV. Thus, when
258 modified by Nd, generally the forbidden zone energy of the material is lower in comparison to
259 non-modified one. That shows the ability to absorb the visible light of these modified materials is

260 greatly improved compared to nano TiO₂ material. For non-modified TiO₂, maximum energy
261 absorption takes place in the ultraviolet radiation region ($\lambda < 400$ nm) with electron excitation from
262 orbital 2p of the O atom the orbital 3d of Ti. Therefore, the E_g value of TiO₂/Nd materials with
263 different Nd contents significantly decreases to below 2.89 eV. As a result, visible light can excite
264 electrons from this intermediate energy level (4f) to the conductive region energy. This is also
265 agreement with the studies on TO₂ modified using rare earth elements (Wojcieszak, Kaczmarek et
266 al. 2012, Wojcieszak, Mazur et al. 2014).

267 **Figure 5.** Eg spectrum of TiO₂/Nd modified nanomaterials with different Nd contents
268 *TiO₂/Nd nanomaterials coated on rice husk ash*

269 The nano TiO₂/Nd modified materials coated on rice husk ash are prepared from sol-gel
270 solution similar to those used to make nano TiO₂/Nd modified materials with a content of 0.36%
271 Nd. Their photocatalytic activity is compared to nano TiO₂ particles. The SEM image of the nano
272 TiO₂/Nd /rice husk ash material shows that on the surface of the material at the crevices and on
273 the holes, there are nano TiO₂/Nd particles that are attached and they are fairly evenly distributed
274 throughout the surface of the rice husk ash. The results also indicate that the coatings on the rice
275 husk ash are homogeneity (see Figure 6).

276 **Figure 6.** SEM images of rice husk ash (a) and nano TiO₂/Nd /rice husk ash (b)

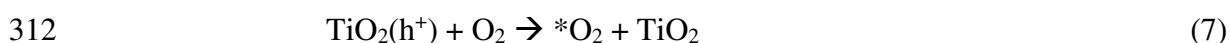
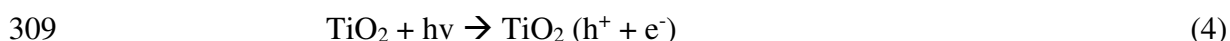
277 **Figure 7.** XRD (a) and EDX (b) spectrum of nano TiO₂/Nd /rice husk ash

278 Figure 7 (a) shows the characterized peaks appeared at the 2θ position = 25.3° of TiO₂, and
279 22° of SiO₂ that indicate the presence of TiO₂ and SiO₂ particles on the surface of nano TiO₂/Nd
280 /rice husk ash material. Mass and percentage of elements found in nano TiO₂/Nd/rice husk ash
281 material are presented in Figure 6 (b). The findings show that the material consists mainly of Si,
282 accounting 83.13%, the O and C make up 6.33 And 5.64%, respectively. However, Ti only
283 occupies a small amount (0.19% w/w), where a small amount of other elements like Nd, K, Cl and
284 Ca are found to derive from rice husk ash. It shows that nano TiO₂/Nd coating rice husk ash
285 material by solgel hydrothermal method has been achieved successfully because of high absorption
286 capacity and photocatalytic activity. Using this material makes the continuous operation of the
287 treatment processing without separating the material after treatment. In addition, it not only
288 increases the removal efficiency but also reduces the treatment cost.

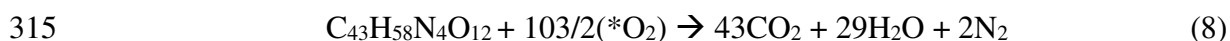
289 **Removal effective of rifampicin of Nd-TiO₂ and Nd-TiO₂/rice husk ash nanomaterials**

290 The result of photocatalytic decomposition of the rifampicin antibiotic in the presence of
 291 TiO₂/Nd and TiO₂/Nd/rice husk ash nanomaterials show in Figure 8. The results clearly show that
 292 both types of materials obtained have photocatalytic activity. However, the activity of TiO₂/Nd
 293 /rice husk ash material is lower (about 10% after 90 min), compared to the decomposition of
 294 rifampicin antibiotics obtained in the case of nano TiO₂/Nd material. This difference is mainly
 295 related to significant differences in the content of nano TiO₂, the light absorption ability, the
 296 rifampicin's absorption capacity onto the rice husk ash material. Although, both materials are
 297 prepared from same size nanoparticles and having the same E_g, the BET surface areas of nano
 298 TiO₂/Nd and TiO₂/Nd/rice husk ash materials are 58.97 and 107 m²/g, respectively. The size of
 299 the TiO₂/Nd /rice husk ash is also much larger than the size of the nano TiO₂/Nd particle. Because
 300 of the bulky molecular structure of rifampicin with many functional groups such as -OH, >NH,
 301 >C=O etc., it can easily make bonds with the metals of the adsorbents. This show more clearly in
 302 the experiment results under the dark conditions (see Figure 8). Also, the very fast absorption rate
 303 can be seen that maximum absorbability is achieved after 15 minutes.

304 Under natural light conditions, the photocatalytic efficiency of both materials increases
 305 markedly over reaction times. However, the rifampicin decomposition efficiency of nano TiO₂/Nd
 306 particles is higher. This is related to the absorption process as well as the size of the rifampicin
 307 molecule. Therefore, the photocatalytic process takes place simultaneously during absorption as
 308 below reactions (Thomas, Radhika et al. 2016).



313 The activated molecules formed will react with the molecules of rifampicin to produce CO₂
 314 and H₂O.



317 From the reaction equation, a large number of activated molecules are needed to oxidize
 318 the C₄₃H₅₈N₄O₁₂, which means a large amount of h⁺ is needed for the reaction.

319

320

321 **Figure 8.** Rifampicin removal efficiency of nano TiO₂/Nd and TiO₂/Nd /rice husk ash
322 under different conditions (TiO₂/Nd-P: nano TiO₂/Nd, natural light; TiO₂/Nd/H-SL:TiO₂/Nd/rice
323 husk ash, natural light; TiO₂/Nd/H-D: TiO₂/Nd /rice husk ash, dark)

324 At an early stage, when Rifampicin molecules are quickly adsorbed to the surface of
325 material, it prevents OH⁻ ion and O₂ molecular interact with the material surface, thereby reducing
326 the formation of activated molecules and facilitating the re-combination of e and hole. Therefore,
327 the rifampicin removal efficiency through photochemical reaction is insignificant. As the reaction
328 time is prolonged, the rates of photochemical reaction of both materials markedly increases. The
329 concentration of rifampicin tends to decrease more significantly for nano TiO₂/Nd materials in
330 comparison to TiO₂/Nd/rice husk ash. This is probably because the rice husk ash accounts for a
331 large proportion of the TiO₂/Nd/rice husk ash material (see SEM and EDX).

332 In the later material, nano TiO₂/Nd particles occupy only a small part of the surface area
333 of the material, therefore, when the rifampicin molecules are absorbed onto the rice husk ash
334 material, the interact between the activated molecules and rifampicin has a lower probability than
335 the nano TiO₂/Nd material. On the other hand, due to the larger size of the TiO₂/Nd/rice husk ash
336 material, it prevents light from going deep into the solution, so the decomposition efficiency is
337 lower and the reaction time lasts longer. When the reaction time lasts up to 90 min, the rifampicin
338 decomposition efficiency of TiO₂/Nd/rice husk ash material reaches about >75%.

339 *Rifampicin degradation kinetics*

340 The results of the kinetic calculations relating to the process of removing rifampicin
341 according to the zero, first and second equations were showed in Figure 9.

342 Summarized results in Table 3 showing that for all 3 kinetics the powder TiO₂/Nd has the
343 highest k-value and regressive correlation, R². The k value in zero kinetic and 1st order kinetics are
344 similar to the maximum and minimum k values, respectively, that were reported in the study of
345 Cizmic et al. (2019) (Cizmic, Ljubas et al. 2019).

346 **Table 3.** Kinetics calculations: reaction rate constant and regression coefficients

347 The Langmuir-Henshilwood kinetics are applied with first-order kinetic similarities as both
348 the absorption process that occurs along with the decomposition reaction take into consideration.
349 Comparison to powder TiO₂/Nd material, TiO₂/Nd material coated with rice husk ash in natural
350 light conditions (-SL) has lower k and R² values, however these were found better than that of

351 TiO₂/Nd/H under dark and UV irradiation. For conditions where the use of UV irradiation the
352 value k is lower than that of natural light may be due to the low intensity of UV radiation and the
353 material has been activated to reduce the forbidden zone energy of material then it can effectively
354 catalyst in the visible area of natural light. In the study of Vaucher et al. (2010), the kinetics of
355 telithromycin photodegradation and oxidative degradation were determined and reported that both
356 photodegradation and oxidative degradation follow first-order reaction kinetics (Vaucher, Paim et
357 al. 2010).

358 Pseudo-first order kinetic model was commonly used in number of studies to investigate
359 the antibiotic degradation process under the different conditions (Zhigang, Wang et al. 2018,
360 Cizmici, Ljubas et al. 2019, Bobirică, Bobirică et al. 2020), photocatalytic degradation of
361 sulfamethazine in aqueous solution using ZnO was reported. The findings showed that 78 and 95%
362 of sulfamethazine were degraded after 60 min irradiation, the rate constant k obtained 2.58×10^{-2}
363 and $4.95 \times 10^{-2} \text{ min}^{-1}$ without and with ZnO, respectively.

364 **Figure 9.** Concentration of rifampicin remaining versus time according to: zero-order reaction
365 (a), first-order reaction (b) and second-order reaction (c)

366 The Langmuir-Henshilwood model was studied by Kais et al (2019) and Safari et al. (2015)
367 for photocatalytic degradation of rifampicin and tetracycline, respectively (Safari, Hoseini et al.
368 2015, Kais, Mezenner et al. 2019). In which, the influence of some parameters and kinetic model
369 were investigated. The results showed that the apparent rate constant (k_{app}) and initial rate constant
370 (r_0) decreased when the initial concentration of rifampicin increased. In some other studies, the
371 amount of photocatalyst (TiO₂) and pH were considered as significant factors affecting the
372 antibiotic degradation process (Radosavljevic, Golubovic et al. 2017, Kais, Mezenner et al. 2019).

374 **Conclusions**

375 Nano TiO₂ materials in the form of anatase are modified with different Nd content by the
376 sol-gel hydrothermic method using a TiCl₄ solution at a temperature of 600°C. The material
377 properties, photocatalytic reactions of the nano TiO₂/Nd and TiO₂/Nd/rice husk ash materials were
378 investigated using modern characteristic techniques. The results showed that Nd doping affects
379 electronic transition energy by changing the width of the forbidden zone. Most notably, the
380 modification enhances the visible light photolytic activity of modified TiO₂ compared to pure
381 TiO₂, and depends on the Nd content. The rifampicin decomposition efficiency of nano Nd-TiO₂
382 material with 0.36% Nd under natural light reaches about 86% after 90 minutes. The TiO₂/Nd/rice

383 husk ash material are successfully prepared when TiO₂/Nd is coated on rice husk ash by the sol-
384 gel hydrothermal method, with the content of Ti in the material about 0.19% (w/w). Although
385 its photocatalytic reaction efficiency to decompose rifampicin is lower than that of nano Nd-TiO₂
386 materials (more than 75% after 90 min), this material is suggested to use because after the
387 photocatalytic process, the Nd-TiO₂ material still remains on the rice husk ash carrier. Therefore,
388 Nd-TiO₂ materials will not release in to solution and not cause secondary environmental pollutants.
389 The Nd-TiO₂/rice husk ash material can be recovered in a simple method and able to be long use.

390 The kinetics of rifampicin removal follows the zero and first-order reaction kinetics
391 especially for TiO₂/Nd-P and TiO₂/Nd/H-SL. The k and R² values of TiO₂/Nd/H-D and
392 TiO₂/Nd/H-UV seem to be similar and remarkable lower than that of powder TiO₂/Nd and
393 TiO₂/Nd/H in solar irradiation.

394
395

396 **REFERENCES**

397
398 Aregu, M. B., S. L. Asfaw and M. M. Khan (2018). " Identification of two low-cost and locally
399 available filter media (pumice and scoria) for removal of hazardous pollutants from tannery
400 wastewater." Environ Syst Res. **7**(1): 10.

401
402 Aregu, M. B., S. L. Asfaw and M. M. Khan (2018). "Identification of two low-cost and locally
403 available filter media (pumice and scoria) for removal of hazardous pollutants from tannery
404 wastewater." Environ Syst Res. **7**(1): 10.

405
406 Bobirică, C., L. Bobirică, M. Râpă, E. Matei, A. M. Predescu and C. Orbeci (2020). "Photocatalytic
407 Degradation of Ampicillin Using PLA/TiO₂ Hybrid Nanofibers Coated on Different Types of
408 Fiberglass." Water **12**: 176.

409
410 Chen, X. and S. S. Mao (2007). "Titanium dioxide nanomaterials: synthesis, properties,
411 modifications, and applications." Chemical Reviews **107**(7): 2891-2959.

412
413 Choi, J. H., S. Maruthamuthu, H. G. Lee, T. H. Ha and J. H. Bae (2009). "Nitrate removal by
414 electro-bioremediation technology in Korean." soil. J Hazard Mater **11**: 1208–1216.

415
416 Cizmic, M., D. Ljubas, M. Rožman, D. Ašperger, L. Curkovic and S. Babic (2019). "Photocatalytic
417 Degradation of Azithromycin by Nanostructured TiO₂ Film: Kinetics, Degradation Products, and
418 Toxicity." Materials **12**: 873.

419
420 Cong, Y., J. Zhang, F. Chen, M. Anpo and D. He (2007). "Preparation, Photocatalytic Activity,
421 and Mechanism of Nano-TiO₂ Co-Doped with Nitrogen and Iron (III)." Journal of Physical
422 Chemistry **111**(28): 10618–10623.

423
424 Du, P. and R. Eisenberg (2012). "Catalysts made of earth-abundant elements (Co, Ni, Fe) for water
425 splitting: Recent progress and future challenges." Energy Environ. Sci. **5**: 6012–6021.

426

427 El-Bahy, Z. M., A. A. Ismail and R. M. Mohamed (2009). "Enhancement of titania by doping rare
428 earth for photodegradation of organic dye (Direct Blue)." Journal of Hazardous Materials **166**:
429 138-143.

430

431 Fukuzumi, S., D. Hong and Y. Yamada (2013). "Bioinspired Photocatalytic Water Reduction and
432 Oxidation with Earth-Abundant Metal Catalysts." J. Phys. Chem. Lett. **4**(20): 3458–3467.

433

434 General statistics office (2018). Press release social and economic situation in 9 months of 2017.

435

436 Hajizadeh, Y., M.-M. Amin, K. Ebrahim and I. Parseh (2018). "Biodeterioration of 1, 1-
437 dimethylhydrazine from air stream using a biofilter packed with compost-scoria-sugarcane
438 bagasse." Atmos Pollut Res. **9**(1): 37–46.

439

440 Huang, C., W. You, L. Dang, Z. Lei, Z. Sun and L. Zhang (2006). "Effect of Nd Doping on
441 Photocatalytic Activity of TiO₂ Nanoparticles for Water Decomposition to Hydrogen." Chin. J.
442 Catal. **27**: 203-209.

443

444 Huang, H., H. Lu, Y. Zhan, G. Liu, Q. Feng and H. Huang (2017). "VUV photo-oxidation of
445 gaseous benzene combined with ozone-assisted catalytic oxidation: effect on transition metal
446 catalyst." Appl Surf Sci. **391**: 662–667.

447

448 Kais, H., N. Y. Mezenner, M. Trari and F. Madjene (2019). "Photocatalytic Degradation of
449 Rifampicin: Influencing Parameters and Mechanism." Russian Journal of Physical Chemistry A.
450 **93**(13): 2834–2841.

451

452 Kumar, A., B. Sengupta, D. Dasgupta, T. Mandal and S. Datta (2015). "Recovery of value added
453 products from rice husk ash to explore an economic way for recycle and reuse of agricultural
454 waste." Reviews in Environmental Science and Bio/Technology **15**(1).

455

456 Kumar, A., S. Singha, D. Dasgupta, S. Datta and T. Mandal (2015). "Simultaneous recovery of
457 silica and treatment of rice mill wastewater using rice husk ash: An economic approach."
458 Ecological Engineering **84**: 29-37.

459

460 Li, X., J. Yu, J. Low, Y. Fang, J. Xiaoc and X. Chen (2015). "Engineering heterogeneous
461 semiconductors for solar water splitting." Journal of Materials Chemistry A **3**: 2485-2534.

462

463 Liu, Y., Y. Guo, Y. Zhu, D. An, W. Gao, Z. Wang, Y. Ma and Z. Wang (2011). "A sustainable
464 route for the preparation of activated carbon and silica from rice husk ash." Journal of Hazardous
465 Materials **186**(2-3): 1314-1319.

466

467 Ma, Y., X. Wang, Y. Jia, X. Chen, H. Han and C. Li (2014). "Titanium Dioxide-based
468 Nanomaterials for Photocatalytic Fuel Generations." Chem. Rev. **114**: 9987.

469

470 Maeda, K. and K. Domen (2007). "New Non-Oxide Photocatalysts Designed for Overall Water
471 Splitting under Visible Light." J. Phys. Chem. C **111**: 7851–7861.

472

473 Nam, N. H., N. H. Hiep, T. T. H. Van and N. T. T. Huong (2016). "Creating nitrogen modified
474 tio2 nano material by urea covered on laterite applying to treat organic compound and bacteria in
475 the outflow of biological treatsystem." Journal of Science of HNUE **61**(9): 93-103.

476

477 Nam, N. H., N. H. Hiep, T. T. H. Van and N. T. T. Huong (2016). "Creating nitrogen modified
478 tio2 nano material by urea covered on laterite applying to treat organic compound and bacteria in
479 the outflow of biological treatsystem." Journal of Science of HNUE **61**(9): 93-103.

480

481 Nguyễn Văn Hưng, Ngô Sỹ Lương, Đặng Thị Thanh Lê and Nguyễn Văn Khanh (2012). "Ảnh
482 hưởng của Nd³⁺ đến cấu trúc và hoạt tính quang xúc tác của bột Nd-TiO₂ kích thước nano điều
483 chế bằng phương pháp thủy nhiệt và thủy phân." Tap chí Khoa học và Công nghệ **50**(3): 367-374.

484

485 Radosavljevic, K. D., A. V. Golubovic, M. M. Radisic, A. R. Mladenovic, D. Ž. Mijin and S. D.
486 Petrovic (2017). "Amoxicillin photodegradation by nano crystalline TiO₂." Chem. Ind. Chem.
487 Eng. Q. **23**(2): 187–195.

488

489 Safari, G. H., M. Hoseini, M. Seyedsalehi, H. Kamani, J. Jaafari and A. H. Mahvi (2015).
490 "Photocatalytic degradation of tetracycline using nanosized titanium dioxide in aqueous solution."
491 Int. J. Environ. Sci. Technol. **12**: 603–616.

492

493 Saucedo-Lucero, J. and S. Arriaga (2015). "Study of ZnO-photocatalyst deactivation during
494 continuous degradation of n-hexane vapors." J Photochem Photobiol A **312**: 28–33.

495

496 Thomas, J., S. Radhika and M. Yoon (2016). "Nd³⁺-doped TiO₂ nanoparticles incorporated with
497 heteropoly phosphotungstic acid: A novel solar photocatalyst for degradation of 4-chlorophenol in
498 water." Journal of Molecular Catalysis A: Chemical **411**: 146-156.

499

500 Vaucher, L. C., C. S. Paim, A. D. Lange and E. E. S. Schapoval (2010). "Degradation Kinetics of
501 Telithromycin Determined by HPLC Method " Journal of Chromatographic Science **48**: 835-839.

502

503 Wanga, C. and D. Astruc (2014). "Nanogold plasmonic photocatalysis for organic synthesis and
504 clean energy conversion." Chem. Soc. Rev. **43**(20): 7188–7216.

505

506 Wen, J., X. Li, W. Liu, Y. Fang, J. Xie and Y. Xu (2015). "Photocatalysis fundamentals and surface
507 modification of TiO₂ nanomaterials." Chinese Journal of Catalysis **36**: 2049–2070.

508

509 Wojcieszak, D., D. Kaczmarek and J. Domaradzki (2012). "Photocatalytic properties of
510 transparent TiO₂ coatings doped with neodymium." Polish Journal of Chemical Technology **14**(3):
511 1-7.

512

513 Wojcieszak, D., M. Mazur, M. Kurnatowska, D. Kaczmarek, J. Domaradzki, L. Kepinski and K.
514 Chojnacki (2014). "Influence of Nd-Doping on Photocatalytic Properties of TiO₂ Nanoparticles
515 and Thin Film Coatings." International Journal of Photoenergy **2014**: 1-10.

516

517 Yang, T., K. Doudrick and P. Westerhoff (2013). "Photocatalytic reduction of nitrate using
518 titanium dioxide for regeneration of ion exchange brine." Water Res. **11**: 1299–1307.

519

520 Zhang, H., X. Ding, X. Chen, Y. Ma, Z. Wang and X. Zhao (2015). "A new method of utilizing
521 rice husk: Consecutively preparing d-xylose, organosolv lignin, ethanol and amorphous superfine
522 silica." Journal of Hazardous Materials **291**: 65-73.

523

524 Zhigang, Y., J. Wang, T. Jiang, Q. Tang and Y. Cheng (2018). "Photocatalytic degradation of
525 sulfamethazine in aqueous solution using ZnO with different morphologies." R. Soc. Open sci. **5**:
526 171457.

527

528

529

530

Figures

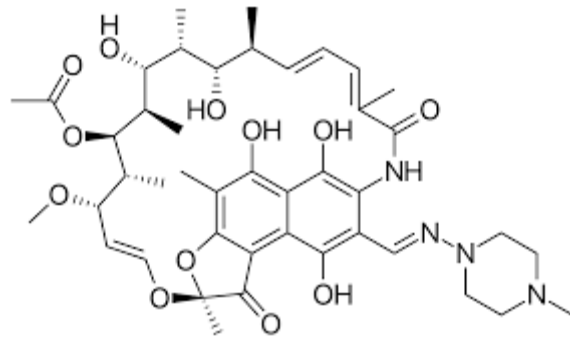


Figure 1. The chemical structure of Rifampicin

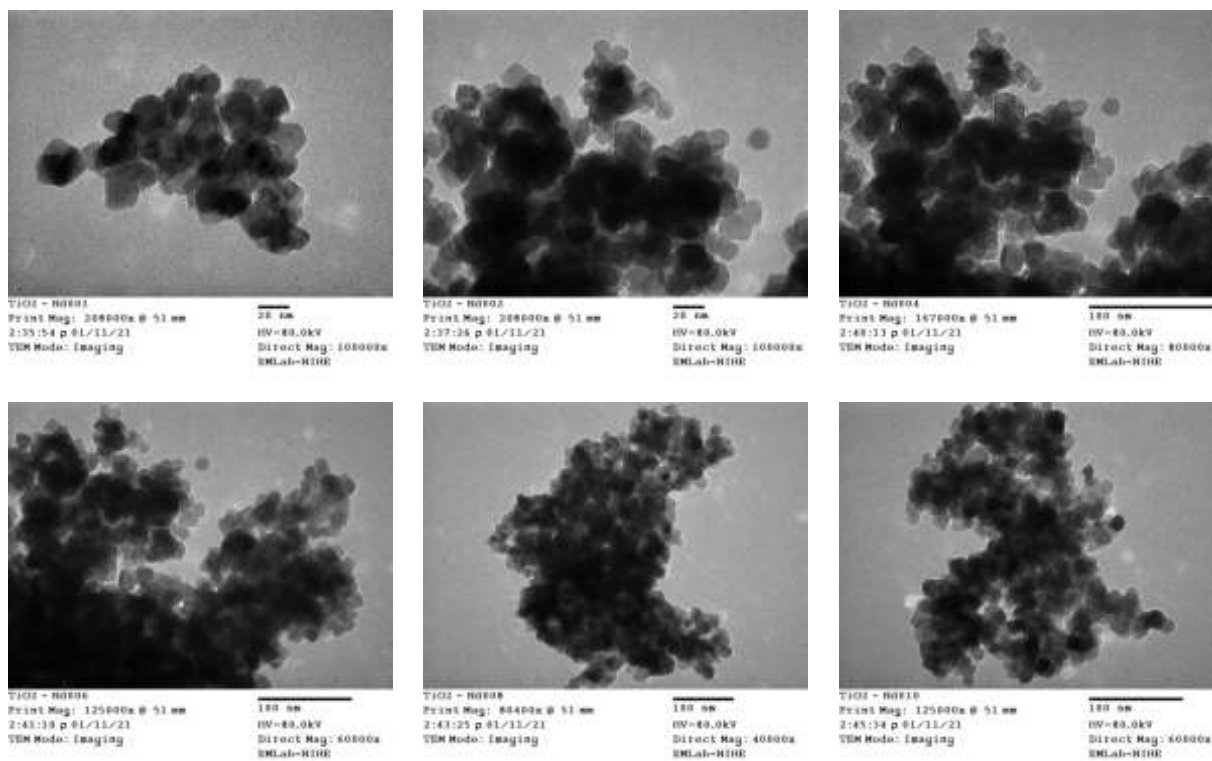


Figure 2. TEM image of TiO₂/Nd modified nanomaterials with different Nd content

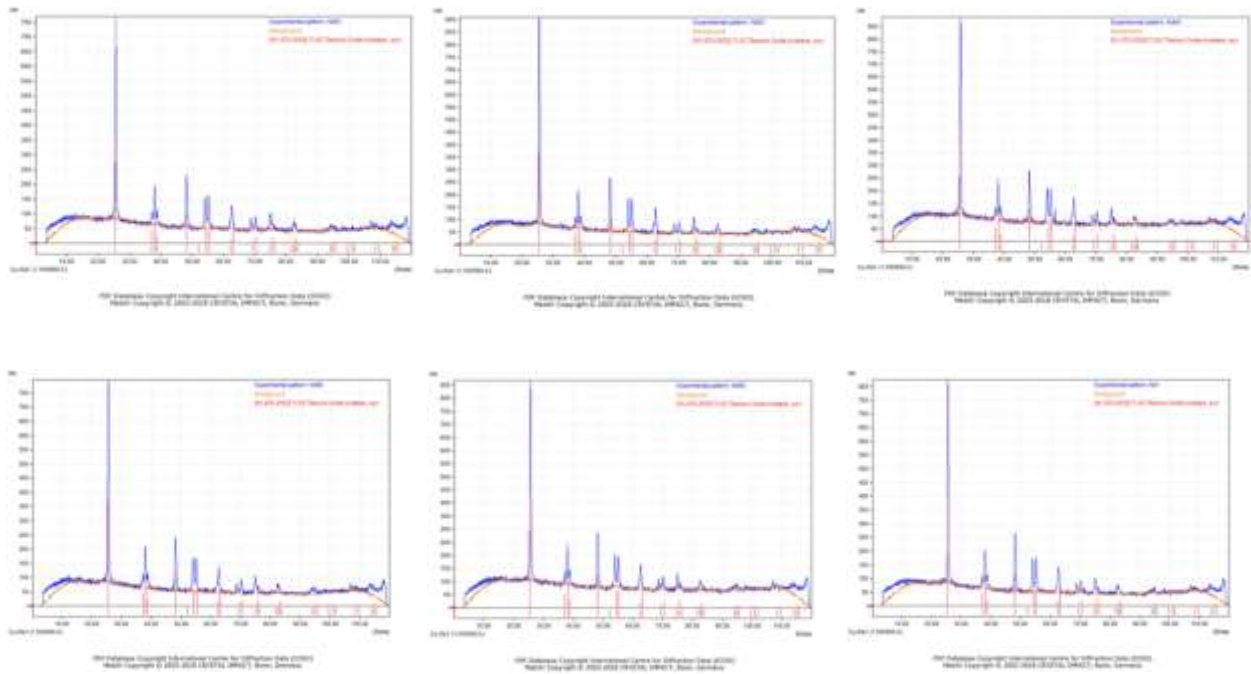


Figure 3. XRD images of nano TiO₂/Nd modified materials with different Nd content

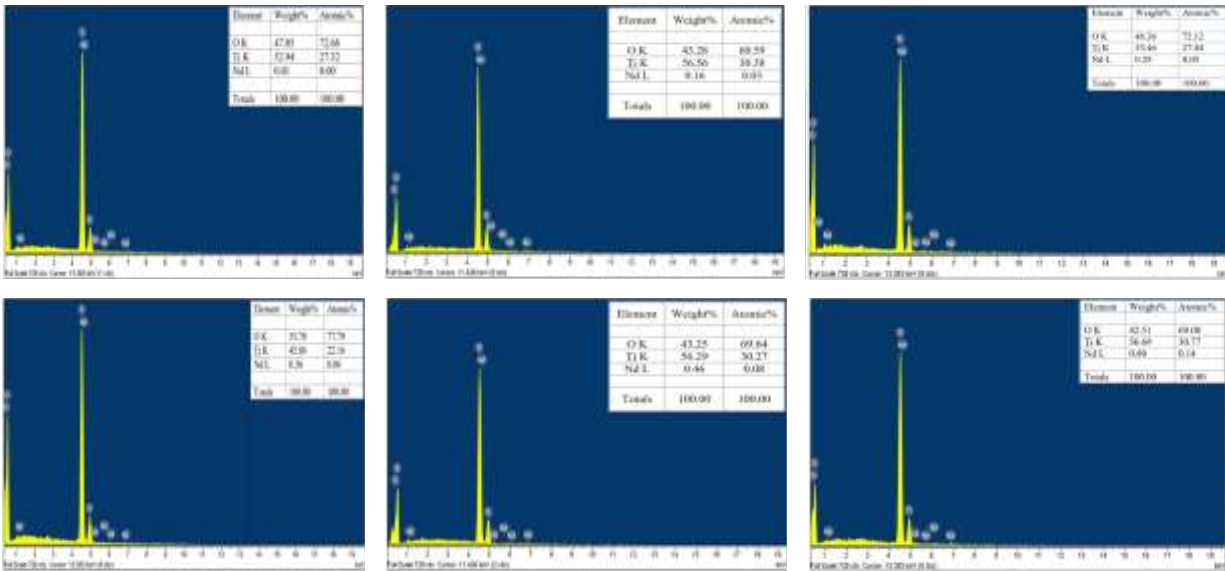


Figure 4. EDX images of TiO₂/Nd modified nanomaterials with different Nd contents

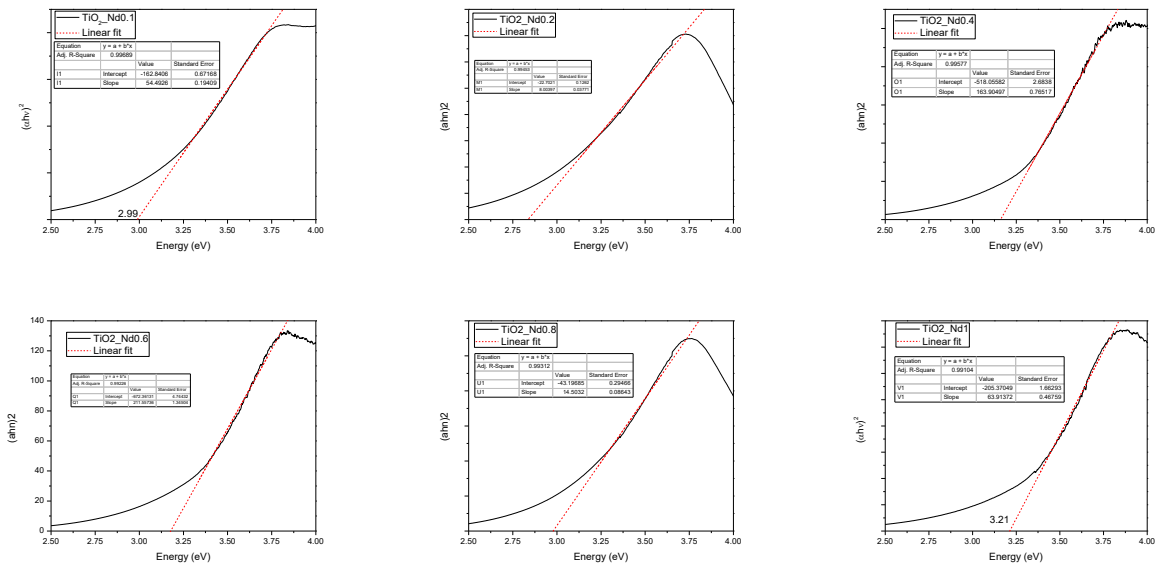
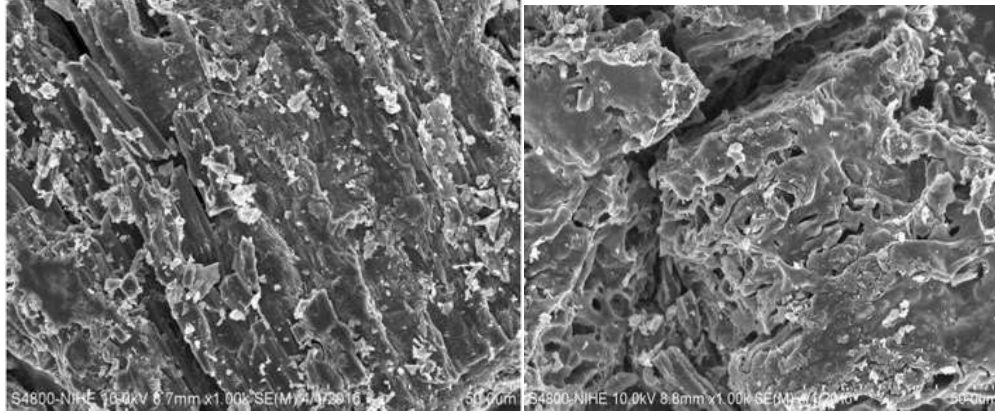


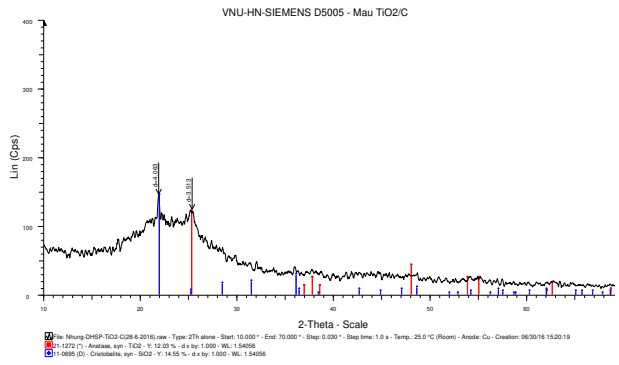
Figure 5. Eg spectrum of TiO₂/Nd modified nanomaterials with different Nd contents



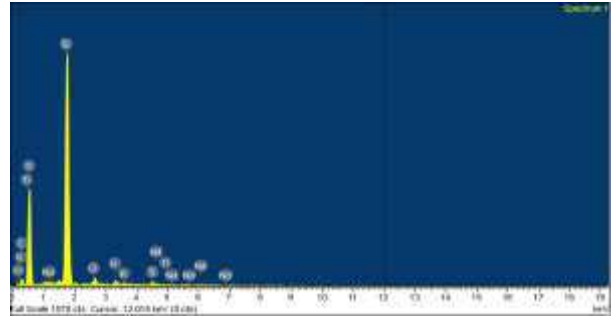
(a)

(b)

Figure 6. SEM images of rice husk ash (a) and nano TiO₂/Nd /rice husk ash (b)



(a)



(b)

Figure 7. XRD (a) and EDX (b) spectrum of nano TiO₂/Nd /rice husk ash

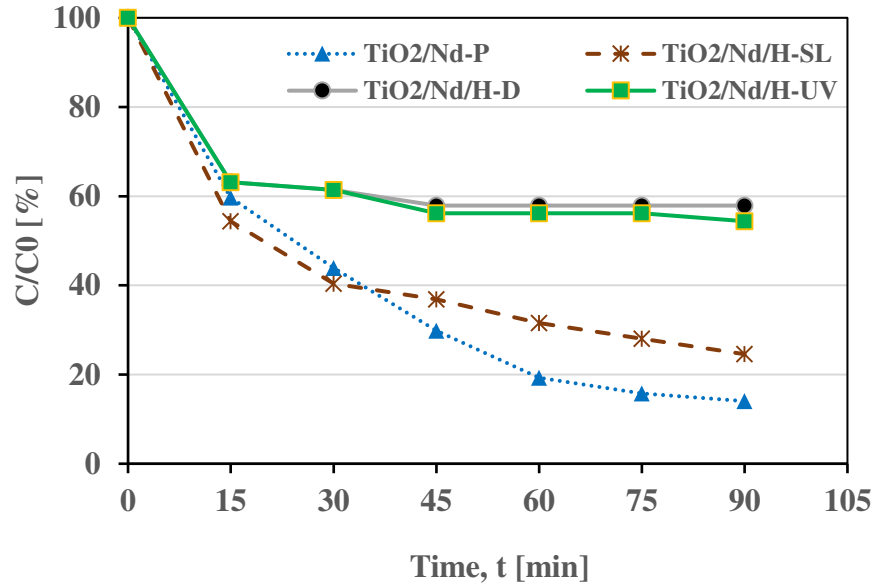


Figure 8. Rifampicin removal efficiency of nano TiO₂/Nd and TiO₂/Nd /rice husk ash under different conditions (TiO₂/Nd-P: nano TiO₂/Nd, natural light; TiO₂/Nd/H-SL: TiO₂/Nd/rice husk ash, natural light; TiO₂/Nd/H-D: TiO₂/Nd /rice husk ash, dark)

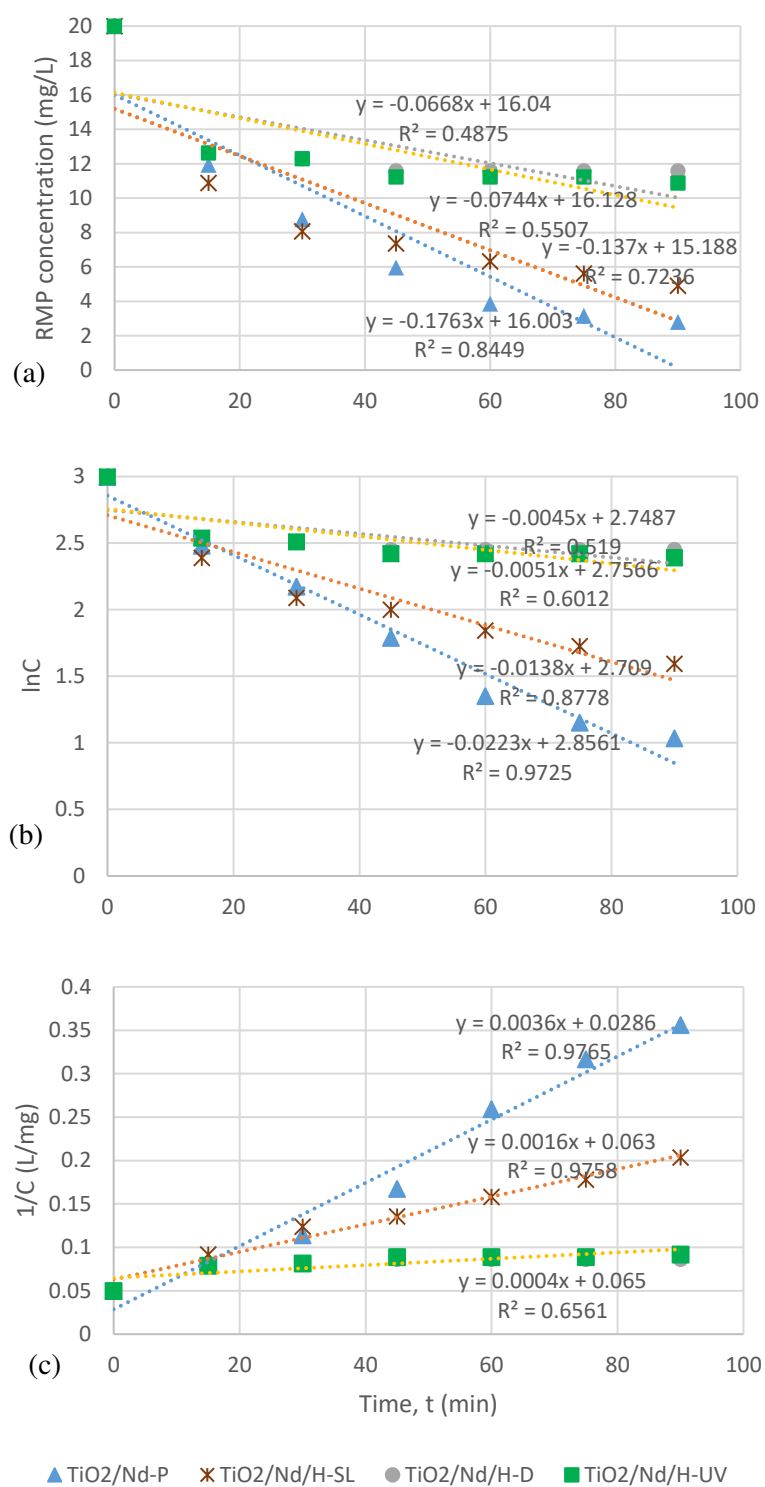


Figure 9. Concentration of rifampicin remaining versus time according to :zero-order reaction (a), first-order reaction (b) and second-order reaction (c)

Tables

Table 1. Composition and rate of chemicals prepared nano TiO₂ modified Nd by the sol-gel hydrothermal method

Chemical	NH ₄ NO ₃ (1.0M)	(NH ₂) ₂ CO (1.0M)	PVA (1.0M)	TiCl ₄ (0.5M)	Nd ³⁺ (1.0g/L)
Volume (ml)	60	450	180	60	0.1-1.0

Table 2. Lattice parameters, particle size and density of *TiO₂/Nd* modified nanomaterials with different Nd content

Nd/TiO ₂ ratio (% w/w)	Samples	Lattice parameters		Density, D (g/cm ³)
		a = b (Å)	c (Å)	
0.01	TiO ₂ - Nd 01	3.770	9.420	3.962
0.16	TiO ₂ - Nd 02			
0.28	TiO ₂ - Nd 04			
0.36	TiO ₂ - Nd 06			
0.46	TiO ₂ - Nd 08			
0.80	TiO ₂ - Nd 1			

Table 3. Kinetics calculations: reaction rate constant and regression coefficients

Materials	Zero order kinetic		1 st order kinetic		2 nd order kinetic	
	k	R ²	k	R ²	k	R ²
TiO ₂ /Nd-P	0.1763	0.85	0.0223	0.97	0.0036	0.98
TiO ₂ /Nd-SL	0.137	0.72	0.0138	0.88	0.0016	0.98
TiO ₂ /Nd/H-D	0.0668	0.49	0.0045	0.52	0.0004	0.66
TiO ₂ /Nd/H-UV	0.0744	0.55	0.0051	0.60	0.0004	0.66